EurJIC European Journal of Inorganic Chemistry

ChemPubSoc Europe

FULL PAPER

DOI:10.1002/ejic.201300969

μ-Chlorido-Bridged Dimanganese(II) Complexes of the Schiff Base Derived from [2+2] Condensation of 2,6-Diformyl-4-methylphenol and 1,3-Bis(3-aminopropyl)tetramethyldisiloxane: Structure, Magnetism, Electrochemical Behaviour, and Catalytic Oxidation of Secondary Alcohols

Mihaela Alexandru,[a] Maria Cazacu,[a] Adina Arvinte,[b] Sergiu Shova,[a] Constantin Turta,[a] Bogdan C. Simionescu,*[a,c] Anatolie Dobrov,[d] Elisabete C. B. A. Alegria,[e,f] Luísa M. D. R. S. Martins,[e,f] Armando J. L. Pombeiro,*[e] and Vladimir B. Arion*[d]

Keywords: Manganese / Template synthesis / Macrocycles / Schiff bases / Oxidation

The reaction of 2,6-diformyl-4-methylphenol with 1,3-bis(3-aminopropyl)tetramethyldisiloxane in the presence of $MnCl_2$ in a 1:1:2 molar ratio in methanol afforded a dinuclear μ-chlorido-bridged manganese(II) complex of the macrocyclic [2+2] condensation product (H_2L), namely, $[Mn_2Cl_2(H_2L)(HL)]Cl{\cdot}3H_2O$ (**1**). The latter afforded a new compound, namely, $[Mn_2Cl_2(H_2L)_2][MnCl_4]{\cdot}4CH_3CN{\cdot}0.5CHCl_3{\cdot}0.4H_2O$ (**2**), after recrystallisation from 1:1 $CHCl_3/CH_3CN$. The coexistence of the free and complexed azomethine groups, phenolato donors, μ-chlorido bridges, and the disiloxane unit were well evidenced by ESI mass spectrometry and FTIR spectroscopy and confirmed by X-ray crystallography. The magnetic measurements revealed an antiferromagnetic interaction between the two high-spin ($S = 5/2$, $g = 2$) manganese(II) ions through the μ-chlorido bridging ligands. The electrochemical behaviour of **1** and **2** has been studied, and details of their redox properties are reported. Both compounds act as catalysts or catalyst precursors in the solvent-free low-power microwave-assisted oxidation of selected secondary alcohols, for example, 1-phenylethanol, cyclohexanol, 2- and 3-octanol, to the corresponding ketones in the absence of solvent. The highest yield of 72% was achieved for 1-phenylethanol by using a maximum of 1% molar ratio of catalyst relative to substrate.

Introduction

The coordination chemistry of manganese with N- and/or O-containing ligands has received attention from researchers owing to the structural diversity of the resulting complexes.[1] Dinuclear manganese(II) complexes are of special interest because of their magnetic properties and as biologically relevant small-molecule model compounds; for example, a Mn catalase[2] has applications in materials science and industrial homogeneous catalysis.[3,4] The interest in bridged polynuclear complexes stems from their significance for understanding the mechanisms of magnetic interactions between metal ions and the synthesis of single-molecule magnets (SMMs).[5] The behaviour of these complexes is mainly dependent on the coordination geometry and binding mode of the ligands as well as on the oxidation state of the manganese ion.[1] Therefore, a large variety of ligands were designed and prepared that can maintain the manganese centres in close proximity or separate them markedly.[6] A number of Schiff bases derived from 2,6-diformyl-4-methylphenol (dfmp) and various amines with NNOO, NON and NOO binding sites have been reported.[7–18] The phenolate-containing ligands are useful models for biological metal binding sites and have the capacity to form metal complexes with interesting magnetic exchange, redox and catalytic properties.[1f,1g,19] Phenolates are also of interest in the design of compartmental ligands

[a] "Petru Poni" Institute of Macromolecular Chemistry, Aleea Gr. Ghica Voda 41 A, Iasi 700487, Romania
http://www.icmpp.ro/staff/bogdansimionescu.html
[b] "Petru Poni" Institute of Macromolecular Chemistry, Centre of Advanced Research in Bionanoconjugates and Biopolymers, Aleea Gr. Ghica Voda 41 A, Iasi 700487, Romania
[c] "Gh. Asachi" Technical University of Iasi, Department of Natural and Synthetic Polymers, Bd. Mangeron 71A, 700050 Iasi, Romania
E-mail: bcsimion@icmp.ro
http://www.icmp.ro/staff/bogdansimionescu.html
[d] Institute of Inorganic Chemistry of the University of Vienna, Währinger Strasse 42, 1090 Vienna, Austria
E-mail: vladimir.arion@univie.ac.at
http://anorg-chemie.univie.ac.at/magnoliaPublic/Research/Bioinorganic-chemistry/Researchers/Arion.html
[e] Centro de Química Estrutural, Instituto Superior Técnico, Universidade de Lisboa, Lisbon, Portugal
E-mail: pombeiro@ist.utl.pt
http://cqe.ist.utl.pt/personal_pages/pages/armando_pombeiro.php
[f] Chemical Engeneering Departmental Area, ISEL, R. Conselheiro Emídio Navarro, 1959-007 Lisboa, Portugal

Supporting information for this article is available on the WWW under http://dx.doi.org/10.1002/ejic.201300969.

able to bind two identical or different metal ions in close proximity.[20–25] Dinuclear μ-chlorido-bridged manganese(II) compounds with N/O donor ligands are relatively rare and only a few six-coordinate manganese(II) compounds have been structurally investigated.[26–29] Only some of these compounds have also been magnetically characterised.[1,26,29b] Catalytic studies on manganese complexes are also scarce.[30]

Quite recently, we reported a new salen-type Schiff base derived from 1,3-bis(3-aminopropyl)tetramethyldisiloxane and substituted 2-hydroxybenzaldehydes. This Schiff base forms copper(II) complexes with a large 12-membered central chelate ring and exhibits catalytic activity in the oxidation of primary and secondary alcohols in the presence of air as oxidant.[31] The choice of the siloxane-containing amine is based on the high flexibility and extremely low polarity of the siloxane moiety.[32] The difference in the polarity between the tetramethyldisiloxane moieties and the amine groups or the azomethine groups that emerge in condensation reactions confers somewhat amphiphilic character to Schiff bases formed and to their metal complexes.

Herein, we report the synthesis of two new μ-chlorido-bridged dimanganese(II) complexes with macrocyclic Schiff bases that resulted from the [2+2] condensation of 2,6-diformyl-4-methylphenol with 1,3-bis(3-aminopropyl)tetramethyldisiloxane (H_2L in Scheme 1) in the presence of $MnCl_2·4H_2O$, namely, $[Mn_2Cl_2(H_2L)(HL)]Cl·3H_2O$ (**1**) and $[Mn_2Cl_2(H_2L)_2][MnCl_4]·4CH_3CN·0.5CHCl_3·0.4H_2O$ (**2**), their solid-state magnetic behaviour and redox properties. Being interested in the metal-catalysed mild oxidative functionalisation of alkanes and alcohols, we also report the oxidation of secondary alcohols to ketones with *tert*-butyl hydroperoxide as oxidant at 80 °C in the absence of solvent with microwave (MW) irradiation with **1** and/or **2** as catalysts or catalyst precursors.

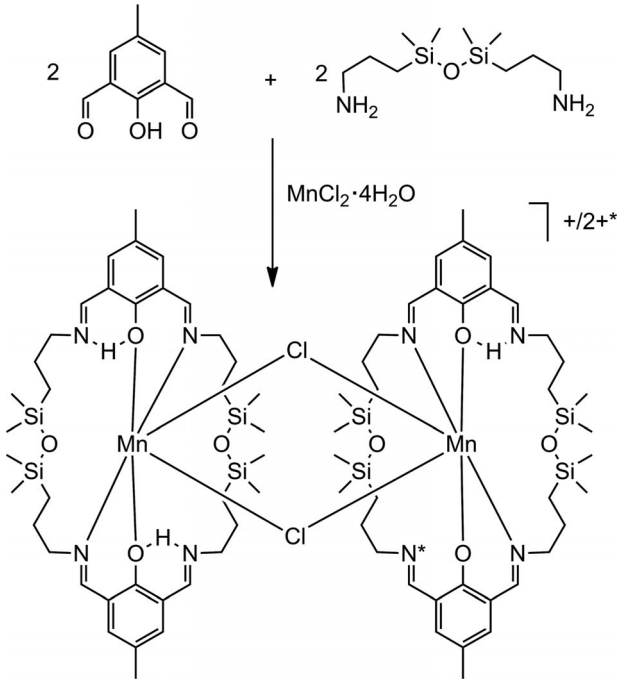

Scheme 1. The reaction to form the dinuclear manganese(II) Schiff base complex $[Mn_2Cl_2(H_2L)(HL)]Cl·3H_2O$ (**1**); in complex **2** the/N* atom is protonated and, therefore, the overall charge of the complex cation is 2+.

Results and Discussion

Synthesis and Characterisation of Metal Complexes

The reaction of 2,6-diformyl-4-methylphenol with 1,3-bis(3-aminopropyl)tetramethyldisiloxane and $MnCl_2·4H_2O$ in a molar ratio of 1:1:2 in methanol afforded a dimanganese(II) complex with macrocyclic [2+2] ligands and two μ-chlorido bridging ligands as shown in Scheme 1. The recrystallisation of $[Mn_2Cl_2(H_2L)(HL)]Cl·3H_2O$ (**1**) from 1:1 chloroform/acetonitrile produced another complex $[Mn_2Cl_2(H_2L)_2][MnCl_4]·4CH_3CN·0.5CHCl_3·0.4H_2O$ (**2**) in 47% yield with **1** as the limiting reagent. By recrystallisation of **1** to form **2**, a marked change of the Mn/ligand/Cl ratio from 2:2:3 in **1** to 3:2:6 in **2** occurs. In addition, the transformation of **1** into **2** is accompanied by a change of the protonation state of one of the ligands from monodeprotonated to neutral.

The formation of a macrocyclic ligand was confirmed by the positive-ion ESI mass spectra of **1** and **2**, which showed the presence of a peak with m/z = 1686 owing to the $[Mn_2Cl_2(H_2L)(HL)]^+$ ion. The isotopic pattern of this peak fits well the theoretical isotopic distribution expected for this ion. Other signals observed at m/z = 842, 806 and 403.5 could be attributed to the ions $[MnCl(H_2L)]^+$, $[Mn(HL)]^+$ and $[Mn(H_2L)]^{2+}$, respectively. In line with these data, in the FTIR spectra of both **1** and **2**, strong absorption bands at 1540 and 1601 cm^{-1} owing to aromatic C=C and C=N stretching vibrations were observed, and no C=O signals at ca. 1700 cm^{-1} were observed.[33] A broad band at ca. 3400 cm^{-1} indicates the presence of cocrystallised water molecules and OH···N groups. The presence of the dimethyl-

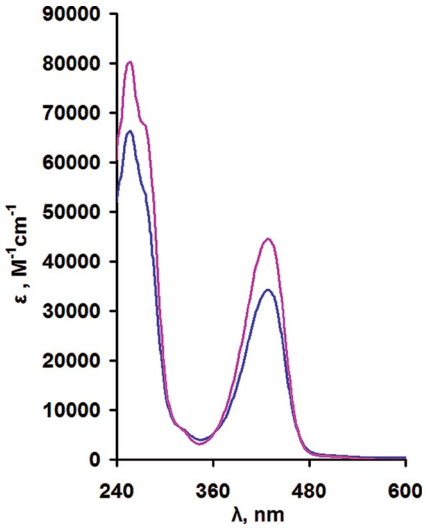

Figure 1. UV/Vis spectra for **1** (blue trace) and **2** (magenta trace) in chloroform.

siloxane unit is evidenced by strong absorptions at 2953 and 2928 cm^{-1}, which correspond to ν_{as} and ν_s (C–H from Si–CH_3), respectively. The bands at 446 and 498 cm^{-1} in **1** might be assigned to ν(Mn–N) and ν(Mn–O), respectively.[4,34,35] The band of ν(Mn–Cl) was observed at 341 cm^{-1} and is characteristic of μ-chlorido-bridged dinuclear complexes.[34] The electronic spectrum of **1** exhibited intense bands at 256 and 429 nm and a shoulder at 274 nm (Figure 1). We assign the strong absorption band at 256 nm to the π–π* transition of the phenol rings, whereas that at 429 nm is attributed to a combination of π–π* transitions of the azomethine chromophore and a ligand-to-metal charge-transfer transition.[21,36,37] The charge transfer may be from the p orbital of the phenolic oxygen atom to the metal d orbitals.[35,38] Analogously, the UV/Vis absorption spectrum of **2** shows intense bands at 256 and 429 nm and a shoulder at 274 nm (Figure 1).

X-ray Crystallography

An X-ray diffraction study has revealed that the crystal structure of **1** consists of a $[Mn_2Cl_2(H_2L)(HL)]^+$ dinuclear cationic species, Cl^- counteranions and cocrystallised water molecules in a 1:1:3 ratio. The structure of $[Mn_2Cl_2(H_2L)(HL)]^+$ (Figure 2) is built up of two six-coordinate Mn^{2+} ions joined into a dinuclear complex by two μ-chlorido bridging ligands and has a Mn1···Mn2 separation of 3.786(1) Å. The four Mn–Cl bond lengths for the bridging μ-chlorido groups fall within the range 2.599(2)–2.618(2) Å, which is in a good agreement with that found for similar bis(μ-chlorido) dimanganese(II) complexes (2.406–2.661 Å).[1,26,28,39–44] Each manganese atom displays a distorted octahedral *cis* geometry (Table 1) and is coordinated by the neutral H_2L (for Mn1) or monodeprotonated HL^- (for Mn2) as tetradentate macrocyclic ligands. A perspective view of the Mn1 coordination site showing the conformation of H_2L is depicted in Figure 3. The coordination environment of Mn1 is formed by the $N_2O_2Cl_2$ donor atoms. The other two imine nitrogen atoms from the H_2L ligand are not coordinated to the metal centre and act as proton donors in hydrogen bonding with the phenolato groups to support the binding mode of the ligand. The geometric parameters of these H bonds are given in the caption to Figure 2. The coordination of a tetradentate N_2O_2 Schiff base ligand results in the formation of two six-membered chelate rings and two 16-membered metallocycles each containing a disiloxane unit. The coordination environment of the Mn2 atom (Figure 2) is very similar to that for Mn1,

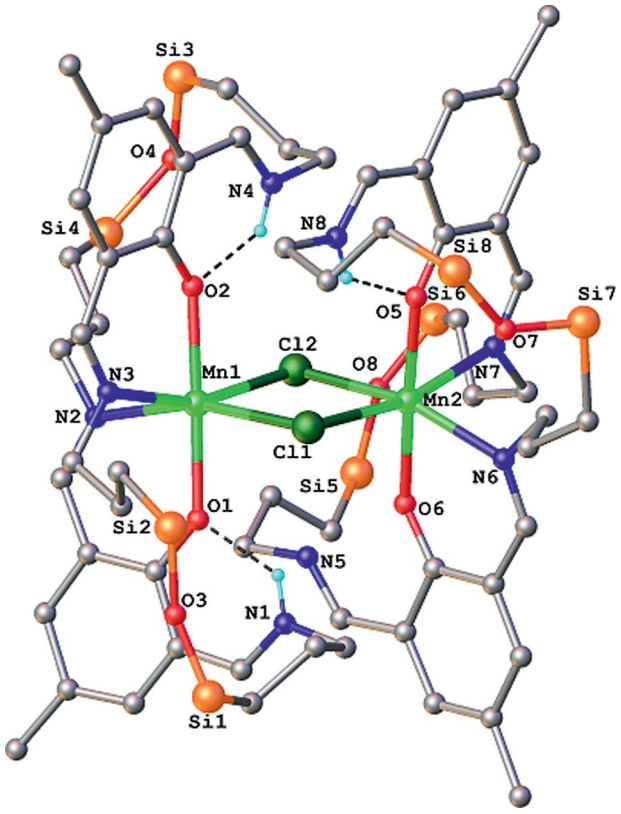

Figure 2. X-ray diffraction structure of a dinuclear cationic complex $[Mn_2Cl_2(H_2L)(HL)]^+$ in the crystal structure of **1**. Three intramolecular H bonds N1–H···O1 [N1–H 0.88 Å, H···O1 1.93 Å, N1···O1 2.601(7) Å, N1–H···O1 131.9°], N4–H···O2 [N4–H 0.88 Å, H···O2 1.91 Å, N4···O2 2.585(7) Å, N4–H···O2 132.1°] and N8–H···O5 [N8–H 0.88 Å, H···O5 1.91 Å, N8···O5 2.596(6) Å, N8–H···O5 133.1°] are also shown.

Table 1. Selected bond lengths [Å] and angles [°] for **1** and **2**.

Atom1–Atom2	**1**	**2**
Mn1–O1	2.084(5)	2.089(4)
Mn1–O2	2.095(5)	2.095(4)
Mn1–N2	2.280(5)	2.292(5)
Mn1–N3	2.301(4)	2.273(5)
Mn1–Cl1	2.599(2)	2.558(2)
Mn1–Cl2	2.606(2)	2.570(2)
Mn2–O5	2.093(4)	2.078(4)
Mn2–O6	2.086(4)	2.088(4)
Mn2–N6	2.284(4)	2.262(5)
Mn2–N7	2.274(4)	2.273(5)
Mn2–Cl1	2.617(2)	2.604(2)
Mn2–Cl2	2.618(2)	2.595(2)
Si1–O3	1.592(6)	1.634(6)
Si2–O3	1.640(6)	1.627(6)
Si3–O4	1.635(7)	1.627(6)
Si4–O4	1.655(7)	1.622(6)
Si5–O8	1.638(5)	1.619(6)
Si6–O8	1.629(5)	1.635(6)
Si7–O7	1.666(5)	1.638(7)
Si8–O7	1.641(5)	1.637(7)
Atom1–Atom2–Atom3		
O1–Mn1–O2	178.6(2)	176.0(2)
O1–Mn1–N2	81.3(2)	80.8(2)
O1–Mn1–N3	99.0(2)	95.0(2)
O2–Mn1–N3	80.5(2)	81.0(2)
N2–Mn1–N3	84.8(2)	85.4(2)
O5–Mn2–O6	178.0(2)	177.7(2)
O6–Mn2–N7	96.2(2)	96.7(2)
O5–Mn2–N7	82.3(2)	81.3(2)
O6–Mn2–N6	81.3(2)	83.0(2)
O5–Mn2–N6	97.3(2)	97.9(2)
N7–Mn2–N6	89.2(2)	86.5(2)
Si1–O3–Si2	157.6(4)	149.0(4)
Si3–O4–Si4	145(1)	152.3(4)
Si7–O7–Si8	147.7(3)	147.8(6)
Si5–O8–Si6	155.9(3)	146.2(4)

but the Schiff base ligand is monodeprotonated (HL^-), the phenolic proton migrates to the noncoordinated azomethine group, as observed for H_2L and analogous ligands in related systems.[45–49] The protons attached to the C=N groups in both H_2L and HL^- were located from a difference Fourier map, and their positional parameters were constrained accordingly. Thus, the charge balance in **1** corresponds to the formulation $[Mn_2Cl_2(H_2L)(HL)]Cl$. Four negative charges provided by three chlorido ligands and one monodeprotonated ligand HL^- are counterbalanced by the four positive charges of two Mn^{2+} ions. The geometrical features of the coordinated ligands confirm the azomethine character of the C–N interatomic bonds in the 2,6-diformyl-4-methylphenol moieties [$C–N_{av}$ 1.299(8) Å] when compared with those from the 1,3-bis(3-aminopropyl)-tetramethyldisiloxane moiety [$C–N_{av}$ 1.462(8) Å]. These parameters along with the C–O bond lengths [$C–O_{av}$ 1.282(7) Å] are in line with those reported for chemically related protonated (neutral) Schiff base ligands.[45–49]

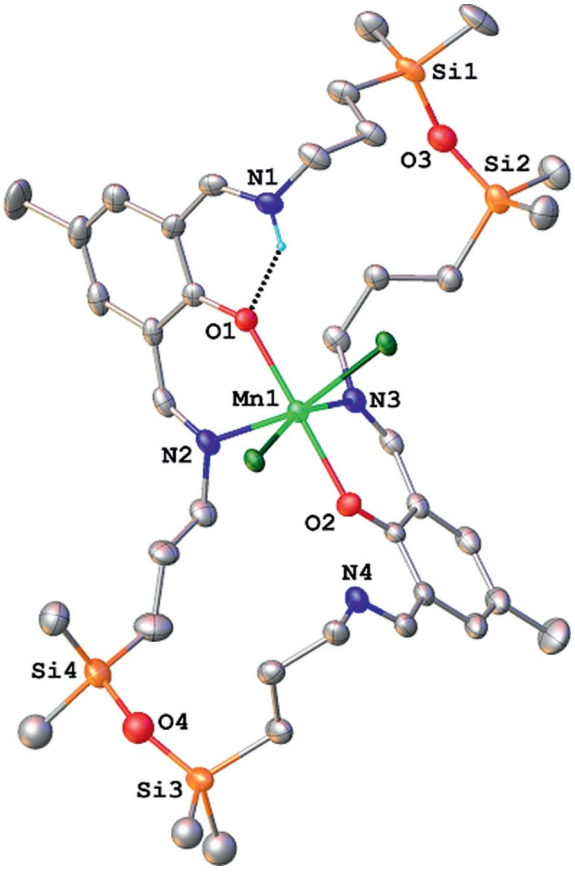

Figure 3. ORTEP plot with thermal ellipsoids at the 40% probability level showing the coordination of H_2L to Mn1 in the crystal structure of **1**. Irrelevant hydrogen atoms are omitted for clarity.

A view of the dinuclear dicationic complex in **2** is shown in Figure 4. The structure of the complex cation resembles that of the dimanganese(II) species found in **1**. One feature of note is that both macrocyclic tetradentate ligands are coordinated to Mn1 and Mn2 as neutral ligands H_2L to form the dicationic complex $[Mn_2Cl_2(H_2L)_2]^{2+}$. All the protonated azomethine groups act as proton donors in H bonds with phenolate oxygen atoms. The parameters of the corresponding H bonds are given in the caption to Figure 4. The doubly positive charge of the dicationic complex is counterbalanced by the anion $[MnCl_4]^{2-}$. The average Mn–Cl distances and Cl–Mn–Cl angles in the dianionic units are 2.359(2) Å and 109.45(8)°, respectively, which fall within the parameters found in related compounds.[50–53]

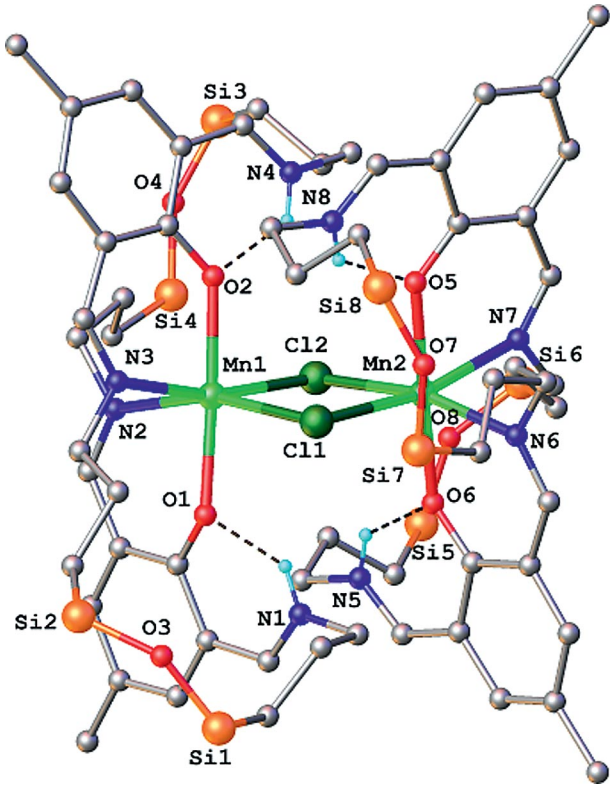

Figure 4. X-ray diffraction structure of a dinuclear complex $[Mn_2Cl_2(H_2L)_2]^{2+}$ in the crystal structure of **2**. Four intramolecular H bonds N1–H···O1 [N1–H 0.88 Å, H···O1 1.93 Å, N1···O1 2.601(7) Å, N1–H···O1 131.9°], N4–H···O2 [N4–H 0.88 Å, H···O2 1.91 Å, N4···O2 2.585(7) Å, N4–H···O2 132.1°], N5–H···O6 [N5–H 0.88 Å, H···O6 1.904 Å, N5···O6 2.588(6) Å], N8–H···O5 [N8–H 0.88 Å, H···O5 1.91 Å, N8···O5 2.596(6) Å, N8–H···O5 133.1°] are also shown.

Thermogravimetric Analysis

Thermogravimetric studies on **1** and **2** were performed in the 25 to 900 °C temperature range under a nitrogen atmosphere (Figure S1). The initial weight loss of 10% in the temperature range 120–300 °C is attributed to the loss of water and solvent molecules. At higher temperature, a further weight loss of ca 40% was observed to 450 °C and is attributed to the pyrolysis of the ligand. The large amount of residue is presumably caused by the formation of metal oxides (MnO and SiO_2).[54] The analysis confirmed the presence of cocrystallised solvent molecules and indicated the optimal temperature for its removal.

Magnetic Measurements

The magnetic susceptibility for a powdered sample of **1** (Mn^{II}_2) was measured in the temperature range 2–300 K under an applied field of 0.1 T. The value of the χT product is 8.70 $cm^3 mol^{-1} K$ at 300 K and corresponds to two uncoupled high-spin ($S_1 = S_2 = 5/2$, $g = 2$) manganese(II) ions (Figure 5).[55] This value remains almost unchanged until ca. 100 K and than continuously decreases with temperature and reaches a value of 2.09 $cm^3 mol^{-1} K$ at 2 K. The temperature dependence of χT indicates an antiferromagnetic interaction between the manganese(II) ions mainly through the μ-chlorido bridging ions. The χT value for **2** (Mn^{II}_2 + Mn^{II}) is ca. 13.81 $cm^3 mol^{-1} K$ at 300 K and has similar temperature dependence: at 2 K χT is 5.54 $cm^3 mol^{-1} K$, which indicates dominant antiferromagnetic Mn^{II}–Mn^{II} interactions within the dinuclear entity of **2** (Figure 5). This temperature dependence of the magnetic properties for both complexes is in good agreement with their crystal structures discussed above. The molar magnetic susceptibility was computed by using the expression derived from the spin-only isotropic exchange Hamiltonian: $H = -JS_1S_2$ ($S_1 = S_2 = 5/2$) and fitted to the experimental data [Equation (1)]. No correction was made for temperature-independent paramagnetism or paramagnetic impurities.

$$\chi_d = \frac{2Ng^2\beta^2}{k(T-\theta)} \times \frac{e^x + 5e^{3x} + 14e^{6x} + 30e^{10x} + 55e^{15x}}{1 + 3e^x + 5e^{3x} + 7e^{6x} + 9e^{10x} + 11e^{15x}},$$
where $x = J/kT$ (1)

For **2**, the additive value for magnetic susceptibility is assumed [Equation (2)].

$$\chi(\mathbf{2}) = \chi_d + \chi(Mn^{II}) \quad (2)$$

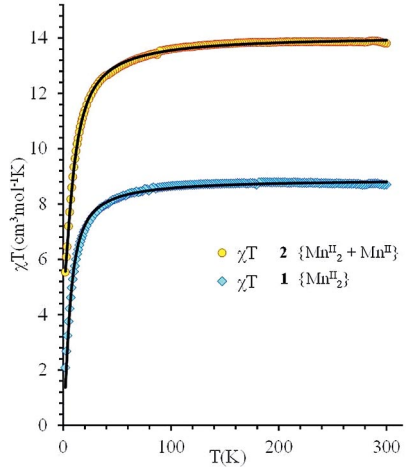

Figure 5. Temperature dependence of the molar values of χT for **1** {Mn^{II}_2} and **2** {Mn^{II}_2 + Mn^{II}}. The solid line is the best least-squares fit to the experimental magnetic data.

The second term in Equation (2) describes the magnetic susceptibility of the $(Mn^{II}Cl_4)^{2-}$ ion, which can be expressed by the Curie–Weiss equation ($S = 5/2$). The coupling between the two paramagnetic $S = 5/2$ ions generates six states of total spin S^* with the following energies E: $S^*(E) = 0(0)$, $1(-J)$, $2(-3J)$, $3(-6J)$, $4(-10J)$, $5(-15J)$. The least-squares fit of the experimental data for **1** and **2** gave the following set of parameters: $g = 2.018(2)$, $J = -0.453(5)$ cm^{-1} for **1**, and $g = 2.074(1)$, $J = -0.708(3)$ cm^{-1} for **2.** The agreement factors $\Sigma(\chi T_{calc} - \chi T_{obs})^2/\Sigma(\chi T_{obs})^2$ are then 5.3×10^{-4} and 8×10^{-5} for **1** and **2**, respectively.

The values of exchange magnetic parameters $J = -0.453(5)$ cm^{-1} for **1** and $J = -0.708(3)$ cm^{-1} for **2** are comparable to those calculated for [Mn_2(2-pyridinemethanol)$_4$(μ-Cl)$_2$Cl$_2$][44] with $J = -0.36$ cm^{-1} and [Mn_2(tacud)$_2$(μ-Cl)$_2$Cl$_2$] (tacud = 1,4,8-triazacycloundecane)[56] with $J = -1.81$ cm^{-1}.

Electrochemical Behaviour of 1 and 2

The redox properties of **1** and **2** as well as, for comparative purposes, $[Me_4N]_2[MnCl_4]$ and benzyltriethylammonium chloride have been investigated by cyclic voltammetry (CV) at a Pt electrode ($d = 1$ mm) in a 0.2 M [nBu$_4$N][BF$_4$]/CH_3CN solution at 25 °C.

Cyclic voltammograms of the di-μ-chlorido-bridged dimanganese(II) complexes **1** and **2** exhibit one two-electron irreversible oxidation process (Figure 6, wave I^{ox}) at $^{I}E_p^{ox}$ = 0.74 and 0.78 V versus the standard calomel electrode (SCE) for **1** and **2**, respectively. These are followed, at higher potential, by a second overall three-electron oxidation (Figure 6, wave II^{ox}) at $^{II}E_{1/2}^{ox}$ = 1.13 and 1.18 V versus SCE for **1** and **2**, respectively. For **2**, a third one-electron irreversible oxidation wave (Figure 6, wave III^{ox} for **2**) is observed at $^{III}E_p^{ox}$ = 1.63 V versus SCE.

For both **1** and **2**, the first two-electron anodic process (I^{ox}) is believed to correspond to the $Mn^{II}/Mn^{II} \rightarrow Mn^{III}/Mn^{III}$ oxidation of the two Mn^{II} centres (Scheme 2).[57]

Exhaustive controlled-potential electrolyses to measure the number of electrons involved in each redox process were not possible owing to fast electrode passivation. However, the involvement of two electrons in the first anodic process (I^{ox}) was deduced from the observed ratio ($2.8 = n^{3/2}$; n is the number of electrons involved, i.e., two in this case) of the current functions $i_pC^{-1}v^{-1/2}$ (i_p = peak current, C = concentration, v = scan rate) calculated for I^{ox} of **2** (or **1**) and for the first one-electron $Mn^{II} \rightarrow Mn^{III}$ anodic process of $[Me_4N]_2[MnCl_4]$ under the same experimental conditions. The cyclic voltammogram of $[Me_4N]_2[MnCl_4]$ (see below) displays two one-electron oxidation waves, the first of which is partially reversible, attributed to the consecutive $Mn^{II} \rightarrow Mn^{III} \rightarrow Mn^{IV}$ processes at $^{I}E_{1/2}^{ox}$ = 1.19 and $^{II}E_p$ = 1.61 V versus SCE. The observed second overall three-electron partially reversible oxidation wave (II^{ox}) in **1** at $^{II}E_{1/2}^{ox}$ = 1.13 V versus the SCE results from the overlap of two different oxidation waves, one assigned to the one-electron irreversible oxidation of the chloride counterion and the second to the two-electron $Mn^{III}Mn^{III}/Mn^{IV}Mn^{IV}$ oxidation process (Scheme 2).

The involvement of the chloride ion oxidation in wave II^{ox} for **1** is supported by the independently measured value

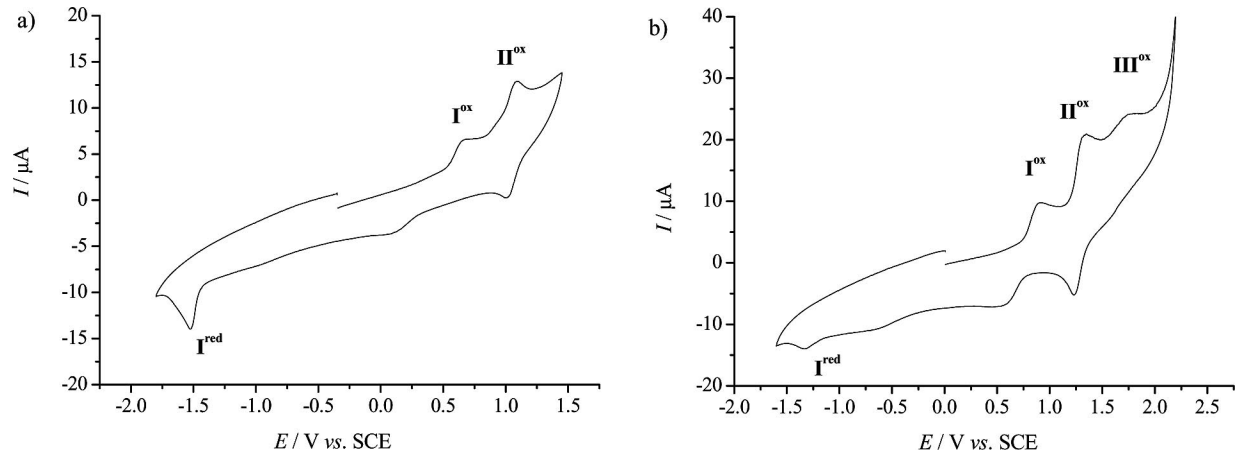

Figure 6. Cyclic voltammogram initiated by the anodic sweep at a Pt electrode of a solution of (a) **1** (1 mM) and (b) **2** (1.4 mM) in 0.2 M [nBu$_4$N][BF$_4$]/MeCN (v = 200 mV/s).

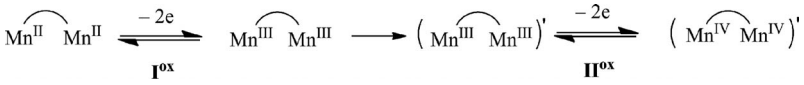

Scheme 2. Oxidation pathways for **1**.

(E_p^{ox} = 1.1 V versus SCE) of the irreversible oxidation wave of benzyltriethylammonium chloride under the same experimental conditions and confirmed by the increase of the current intensity of the wave II^{ox} upon the addition of this chloride salt to a solution of **1**.

For **2**, the observed second overall three-electron partially reversible oxidation wave (Figure 6, II^{ox}) also concerns the involvement of two different oxidation processes, the single electron oxidation of the counterion $[MnCl_4]^{2-}$ (see above) and the $Mn^{III}Mn^{III}/Mn^{IV}Mn^{IV}$ two-electron oxidation.

The irreversible third anodic process observed for **2** (Figure 6, b, III^{ox}) is attributed to the $Mn^{III} \rightarrow Mn^{IV}$ oxidation of the counterion $[MnCl_4]^{2-}$ (vide supra). Moreover, the involvement of the oxidation of $[MnCl_4]^{2-}$ in waves II^{ox} and III^{ox} for **2** was confirmed by the addition of $[NMe_4]_2[MnCl_4]$, which resulted in the increase of such oxidation waves. The difference between the oxidation potentials of the II^{ox} and I^{ox} waves in **1** and **2** ($^{II}E_{1/2}^{ox} - {}^{I}E_p^{ox} \approx 0.4$ V) is comparable to that (0.45 V) observed in $(Et_3NH)_2[\{Mn(TPA)\}_2(\mu\text{-}Cl)_2](ClO_4)_4$ [TPA = tris(2-pyridylmethyl)amine] for the same redox pairs $Mn^{IV}Mn^{IV}/Mn^{III}Mn^{III}$ and $Mn^{III}Mn^{III}/Mn^{II}Mn^{II}$.[57]

Upon scan reversal, after the first oxidation wave I^{ox} (for **1** and **2**), one irreversible reduction process (I^{red}) is detected at $E_p^{red} \approx -1.4$ V versus SCE and is conceivably caused by the reduction of a new species, denoted by $(Mn^{III}Mn^{III})'$ in Scheme 2, formed at the anodic wave (I^{ox}). This indicates that the dinuclear Mn^{III}/Mn^{III} species, formed at the first anodic process in **1** and **2**, is unstable. The partial reversibility of the second oxidation wave (II^{ox}) is preserved even at low scan rates, and the current function $i_pC^{-1}v^{-1/2}$ does not vary appreciably within the studied scan rate range (50 mV s^{-1} to 4 V s^{-1}), which is consistent with the involvement of a constant number of electrons.

The occurrence of both (Mn^{II}/Mn^{III}) oxidations at identical potentials at the oxidation wave I^{ox}, that is, without differentiation of the potentials of the $Mn^{II}Mn^{II}/Mn^{II}Mn^{III}$ and $Mn^{II}Mn^{III}/Mn^{III}Mn^{III}$ redox pairs, indicates that the mixed-valence $Mn^{II}Mn^{III}$ species is rather unstable and the μ-chlorido bridging ligands, in our complexes, isolate the metal atoms from each other electronically, which results in an undetectable (by CV) electronic interaction. Similarly, a rather weak Mn–Mn interaction was proposed for the μ-dichlorido-bridged dimanganese(II) compound $[\{MnCl(bpea)\}_2(\mu\text{-}Cl)_2]$ [bpea = *N*,*N*-bis(2-pyridylmethyl)ethylamine].[30] However, stronger interactions have been reported for other μ-chlorido-bridged species such as $[\{MnCl(dipa)\}_2(\mu\text{-}Cl)_2]$ [dipa = dipyridylmethylamine][58] and $(Et_3NH)_2[\{Mn(TPA)\}2(\mu\text{-}Cl)_2](ClO_4)_4$,[57] which exhibit distinct $Mn^{II}Mn^{II}/Mn^{II}Mn^{III}$ and $Mn^{II}Mn^{III}/Mn^{III}Mn^{III}$ oxidations waves.

Catalytic Oxidation of Secondary Alcohols

Complexes **1** and **2** have been tested as catalysts (or catalyst precursors) for the oxidation of common secondary alcohols (mainly 1-phenylethanol) to the respective ketones with *tert*-butyl hydroperoxide (*t*BuOOH, TBHP; 2 equiv.) as oxidising agent under typical conditions of 80 °C, microwave (MW) irradiation, 3 h reaction time and in the absence of any added solvent (Scheme 3 for the oxidation of 1-phenylethanol). Selected results are summarised in Table 2.

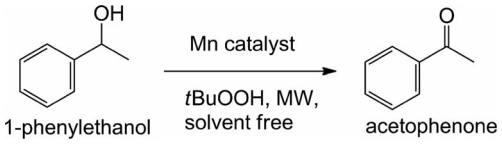

Scheme 3. Solvent-free oxidation of 1-phenylethanol to acetophenone.

Table 2. Oxidation of selected secondary alcohols with **1** or **2** as catalyst precursors.[a]

Entry	Catalyst	Substrate	Catalyst amount [mol-% vs. substrate]	TON[b]	Yield[c] [%]
1	**1**	1-phenylethanol	0.02	238	5
2	**1**	1-phenylethanol	0.04	185	8
3	**1**	1-phenylethanol	0.1	122	12
4	**1**	1-phenylethanol	0.2	113	22
5	**1**	1-phenylethanol	0.4	82	36
6	**1**	1-phenylethanol	0.8	78	66
7	**1**	1-phenylethanol	1.0	72	72
8	**1**	1-phenylethanol	1.4	66	74
9[d]	**1**	1-phenylethanol	0.4	83	30
10[e]	**1**	1-phenylethanol	0.4	13	5
11[f]	**1**	1-phenylethanol	0.1	46	15
12[g]	**1**	1-phenylethanol	0.1	99	38
13[h]	**1**	1-phenylethanol	0.4	5	2
14[i]	**1**	1-phenylethanol	0.4	121	57
15[j]	**1**	1-phenylethanol	0.4	51	34
16[k]	**1**	1-phenylethanol	0.4	94	20
17[l]	**1**	1-phenylethanol	0.4	107	42
18	**1**	cyclohexanol	0.4	21	39
19	**1**	2-octanol	0.4	89	28
20	**1**	3-octanol	0.4	44	15
21	**2**	1-phenylethanol	0.02	310	6
22	**2**	1-phenylethanol	0.1	99	10
23	**2**	1-phenylethanol	0.2	187	18
24	**2**	1-phenyethanol	0.4	81	37
25[m]	$[Me_4N]_2[MnCl_4]$	1-phenylethanol	0.8	15	12
26[m]	$MnCl_2$	1-phenylethanol	0.8	9	7

[a] Reaction conditions: 5 mmol of substrate, 1–70 μmol of catalyst (0.02–1.4 mol-% vs. substrate), 10 mmol of TBHP (2 equiv.), 80 °C, 3 h reaction time, microwave irradiation (10 W). [b] Turnover number = number of mol of product per mol of catalyst. [c] Mol of ketone product per mol of alcohol. [d] 20 mmol of TBHP (4 equiv.). [e] H_2O_2 30% aqueous solution instead of TBHP. [f] T = 50 °C. [g] T = 90 °C. [h] In the presence of Ph_2NH (10 mmol). [i] In the presence of TEMPO (5 mol-% vs. substrate). [j] In MeCN. [k] In H_2O. [l] In K_2CO_3 aqueous solution (1 M). [m] Included for comparative purposes.

The effect of the amount of catalyst **1** was studied for the 1-phenylethanol oxidation (Table 2, Entries 1–8; Figure 7). An increase from 1 (0.02 mol-% vs. substrate) to 70 μmol (1.4 mol-% vs. substrate) resulted in a yield enhancement from 5 to 74%. However, beyond 50 μmol of catalyst, the yield remained almost unchanged. As expected, the increase of the catalyst amount resulted in a decrease of the turnover number (TON; mol of product/mol of catalyst) from 238 to 66 as the amount of catalyst changed from 0.02 to 1.4 mol-% versus substrate (Table 2, Entries 1 and 8). The use of more oxidant does not lead to a better conversion (Table 2, Entries 5 and 9). Blank tests (in the absence of any catalyst) were performed under common reaction conditions and no significant conversion was observed (<0.5%).

Microwave irradiation (MW) can provide a more efficient synthetic method than conventional heating and allows the attainment of similar yields in shorter times, improved yields and/or selectivities.[59–63] A favourable effect of MW is also observed in this study, even with the low power of 10 W, as reported for other systems.[60–62] Hence, for example, only 6% of product yield was obtained after 3 h reaction under the same conditions as those of Table 2, Entry 5 (36% yield) with conventional heating (oil bath). After 15 h reaction, 58 and 17% yields were obtained for MW and conventional heating, respectively. Higher microwave power (from 10 to 40 W) does not show a significant yield enhancement, as once the desired temperature is achieved, the power decreases automatically to values below 10 W.

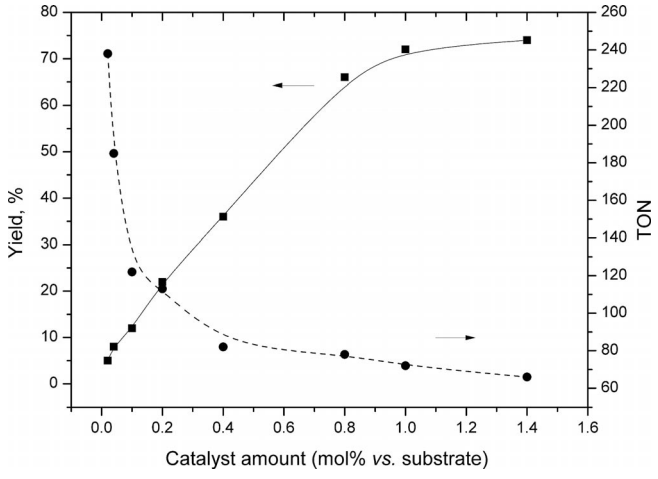

Figure 7. Effect of the amount of catalyst **1** (0.02–1.4 mol-% vs. substrate) on the yield and TON for the oxidation of 1-phenylethanol to acetophenone, 80 °C, 3 h.

The use of hydrogen peroxide (30% aqueous solution) instead of TBHP results in a large decrease in the yield from 36 to 5% (Table 2, Entries 5 and 10), in accord with the expected decomposition of H_2O_2 under the reaction condi-

tions (80 °C). The temperature is an important factor, as the reaction proceeds more efficiently at higher temperatures. Attempts to perform the oxidation of 1-phenylethanol in the presence of **1** at room temperature failed, whereas the reaction conducted at 50 °C resulted in a marked acetophenone yield drop relative to that at 80 °C (from 36% at 80 °C to 15% at 50 °C; Table 2, Entries 5 and 11). The ketone yield does not increase significantly above 80 °C (from 36% at 80 °C to 38% at 90 °C; Table 2, Entries 5 and 12).

Performing the reaction in acetonitrile (5 mL) does not change significantly the yield, for example, the 1-phenylethanol oxidation in the presence of **1** (Table 2, Entries 5 and 15), whereas the addition of the same volume of water results in a significant yield reduction from 36 to 20% (Table 2, Entry 16; Figure 8) under the same reaction conditions. On the contrary, the use of a basic 1 M solution of K_2CO_3 (Table 2, Entry 17; Figure 8) results in a significant increase of the conversion of the alcohol to the ketone compared to the reaction in water (from 20% in water only to 42% in basic solution). The role of basic additives, which facilitate the deprotonation of the alcohol was demonstrated previously.[64,65]

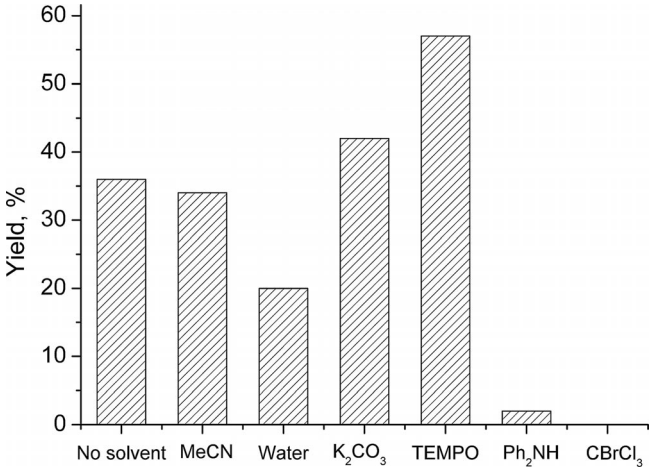

Figure 8. Influence of different solvents (MeCN, H_2O) and additives (1M K_2CO_3, TEMPO, radical traps) on the yield of acetophenone from oxidation of 1-phenylethanol.

Other secondary alcohols were also tested, in particular cyclohexanol, and similar results were obtained, that is, the oxidation of cyclohexanol yielded 39% of cyclohexanone (Table 2, Entry 18), which is comparable to the 36% yield (Table 2, Entry 5) obtained for 1-phenylethanol under the same reaction conditions (20 μmol, 80 °C, MW, 3 h).

Linear aliphatic alcohols, namely 2-octanol and 3-octanol, lead to lower yields under similar reaction conditions, as reported in other cases.[60,63,65a] Thus, the oxidation of 2-octanol and 3-octanol yield 28 and 18% of the respective ketones, 2-octanone and 3-octanone, in 3 h.

The relevance of the H_2L and HL ligands on the catalytic activity of **1** and **2** is shown by the catalytic performances of $[Me_4N]_2[MnCl_4]$ and $MnCl_2$ in the oxidation of 1-phenylethanol compared with those of **1** and **2** under the same reaction conditions. The oxidation of that alcohol (5 mmol) at 80 °C in the presence of the same metal molar amount (40 μmol of Mn) of the Mn compound led to much lower yields of acetophenone after 3 h in the cases of $[Me_4N]_2$-$[MnCl_4]$ and $MnCl_2$ (12 and 7%, respectively; Table 2, Entries 25 and 26) than for **1** and **2** (36 and 37%, Table 2, Entries 5 and 24). The similar results obtained for **1** and **2** and the lower performance of $[Me_4N]_2[MnCl_4]$ show that the $[MnCl_4]^{2-}$ counterion present in **2** does not have a dominant influence on the catalytic activity.

The addition to the reaction mixture of Ph_2NH or $CBrCl_3$, well known oxygen- or carbon-radical traps, respectively,[66,67] led to a large yield drop of over 90%, compared to the reaction under the same conditions (20 μmol, 80 °C, MW, 3 h) in the absence of a radical trap. This result suggests the generation of oxygen and carbon radicals in the reaction, which are trapped by those radical scavengers. A possible mechanism[64h,64i,65a,65d] for this system may involve coordination of the alcohol PhCH(OH)-Me (with deprotonation to form the alkoxide ligand) and 2,2,6,6-tetramethylpiperidyl-1-oxyl (TEMPO) radical, followed by H transfer from the former to the latter to form the *O*-ligated radical $PhC^{\cdot}(O)Me^{-}$ and TEMPOH. Intramolecular electron-transfer from coordinated $PhC^{\cdot}(O)Me^{-}$ to the Mn^{II} ion leads to the formation of the ketone PhC(O)-Me and Mn^{I} ion, which is reoxidised to Mn^{II} by O_2/*t*BuOOH. The TEMPO radical is also regenerated upon oxidation of TEMPOH.

To increase the activity of **1** in solvent-free MW-assisted peroxidative oxidation of 1-phenylethanol, we have investigated the influence of TEMPO, a nitroxyl radical that promotes the oxidation catalysis of alcohols.[60,65a,65c,65d,68–71] Recently, some of us reported on several efficient systems involving copper(II) triazapentadienate,[60,63] bis- and tris-pyridyl amino and imino thioether Cu and Fe complexes[61] for the MW-assisted oxidation of secondary alcohols to the corresponding ketones, as well as the in situ generated copper(II)-diimine complexes toward the TEMPO-mediated oxidation of benzylic alcohols in aqueous media[65a] and Cu^{II} complexes containing arylhydrazones from methylene-active nitriles toward the selective oxidation of primary and secondary alcohols to the corresponding carbonyl compounds.[60] Other manganese-based systems were applied for alcohol oxidation, namely, silica-supported manganese dioxide (MnO_2) in the oxidation of benzyl alcohol under solvent-free conditions,[72] which yielded 88% of acetophenone under MW for 20 s. However, this system required excess MnO_2 relative to the substrate (5:1 molar ratio), whereas in the present study we have achieved 72% yield by using a maximum of 1% molar ratio of catalyst relatively to substrate. Furthermore, mixed Mn–Cu or Mn–Co nitrates[70] and heterogeneous Cu–Mn mixed oxides[71] in combination with TEMPO have been employed for the selective aerobic oxidation of a variety of alcohols to the corresponding aldehydes and ketones under mild conditions. In our case, a significant yield increase was observed for the 1-phenylethanol oxidation in the presence of **1** (from 36% in the absence of TEMPO to 57% in its presence; Table 2, Entries 5 and 14).

Conclusions

Two new μ-chlorido-bridged dimanganese(II) complexes of the Schiff base derived from 2,6-diformyl-4-methylphenol and 1,3-bis(3-aminopropyl)tetramethyldisiloxane in the presence of $MnCl_2$, $[Mn_2Cl_2(H_2L)(HL)]Cl{\cdot}3H_2O$ (**1**) crystallised from methanol or $[Mn_2Cl_2(H_2L)_2][MnCl_4]{\cdot}4CH_3CN{\cdot}0.5CHCl_3{\cdot}0.4H_2O$ (**2**) crystallised from **1** in a chloroform/acetonitrile mixture, have been obtained. The complexes were well-characterised by elemental analysis, ESI mass spectrometry and spectroscopic methods. The FTIR spectroscopy and ESI mass spectra emphasise the coexistence of the free and complexed azomethine and phenolato groups, μ-chlorido bridges and siloxane unit. The structures of the complexes have been determined by single-crystal X-ray diffraction. The magnetic measurements revealed two high-spin (S = 5/2, g = 2) Mn^{II} ions and an antiferromagnetic interaction between them through bridging μ-chlorido ligands. Complexes **1** and **2** act as catalysts or catalyst precursors for the oxidation of selected secondary alcohols, such as 1-phenylethanol, cyclohexanol, 2- and 3-octanol, to the respective ketones with *tert*-butyl hydroperoxide as oxidant at 80 °C with low-power microwave irradiation and a moderate reaction time. The effect of different factors (catalyst and/or oxidant amount, temperature, solvent, presence of a base, etc.) on the efficiency of catalytic conversion of 1-phenylethanol into acetophenone has been elucidated. A maximum yield of 72% was achieved with a 1% molar ratio of **1** relative to substrate.

Experimental Section

Materials: All chemicals were obtained from commercial sources and used as received. 2,6-Diformyl-4-methylphenol (99% purity, m.p. 129–131 °C) was purchased from Polivalent-95. 1,3-Bis(3-aminopropyl)tetramethyldisiloxane was received from Alfa Aesar, and $MnCl_2{\cdot}4H_2O$ was purchased from Sigma–Aldrich.

Synthesis of Complexes

$[Mn_2Cl_2(H_2L)(HL)]Cl{\cdot}3H_2O$ (1): A solution of 1,3-bis(3-aminopropyl)tetramethyldisiloxane (0.61 g, 2.45 mmol) in methanol (5 mL) was added dropwise to a solution of 2,6-diformyl-4-methylphenol (0.40 g, 2.44 mmol) in methanol (7.5 mL) and dichloromethane (2 mL), and the resulting mixture was heated to reflux for 2 h. Then, a solution of $MnCl_2{\cdot}4H_2O$ (0.97 g, 4.9 mmol) in methanol (9.5 mL) was added, and the mixture was heated to reflux for 24 h. The solution was filtered, and the resulting solution was allowed to stand at room temperature to produce orange crystals, which were separated after 3 d, washed with cold methanol and dried in air, yield 0.75 g, 17.0%. $C_{76}H_{133}Cl_3Mn_2N_8O_{11}Si_8$ (1775.84): calcd. C 51.40, H 7.55, N 6.31; found C 51.29, H 7.37, N 6.10. FTIR (KBr): $\tilde{\nu}$ = 3441 (s), 2953 (s), 2870 (m), 1653 (vs), 1623 (s), 1609 (m), 1540 (vs), 1493 (s), 1456 (m), 1409 (m), 1362 (m), 1254 (s), 1231 (m), 1184 (m), 1069 (s), 987 (m), 838 (s), 783 (s), 707 (m), 629 (w), 590 (w), 566 (m), 552 (w), 544 (w), 536 (w), 528 (w), 521 (w), 498 (m), 491 (m), 482 (m), 474 (m), 458 (w), 429 (w), 421 (w), 414(w) cm^{-1}. UV/Vis ($CHCl_3$): λ_{max} (ε, $M^{-1}cm^{-1}$) = 256 (6.63×10^4), 274 (5.42×10^4), 429 (3.43×10^4) nm.

$[Mn_2Cl_2(H_2L)_2][MnCl_4]{\cdot}4CH_3CN{\cdot}0.5CHCl_3{\cdot}0.4H_2O$ (2): Complex **1** (0.5 g, 0.28 mmol) was dissolved in a 1:1 $CHCl_3/CH_3CN$ mixture (10 mL). Orange crystals suitable for X-ray diffraction data collection formed in one week, yield 0.28 g, 47.0% (with **1** as the limiting reagent). The product was collected by filtration and dried in vacuo at 125 °C for 4 h to give solvent-free $[Mn_2Cl_2(H_2L)_2][MnCl_4]$. $C_{76}H_{128}Cl_6Mn_3N_8O_8Si_8$ (1884.09): calcd. C 48.45, H 6.85, N 5.95; found C 48.10, H 6.98, N 5.71. FTIR (KBr pellet): $\tilde{\nu}$ = 3437 (m), 2953 (s), 2924 (m), 1653 (vs), 1628 (s), 1609 (m), 1541 (vs), 1495 (s), 1456 (m), 1449 (m), 1412 (w), 1385 (w), 1385 (s), 1362 (m), 1329 (w), 1254 (s), 1231 (m), 1182 (m), 1065 (s), 988 (m), 878 (m), 837 (s), 820 (s), 781 (s), 745 (w), 708 (w), 679 (w), 669 (w), 565 (w), 498 (w), 474 (w), 446 (w) cm^{-1}. UV/Vis ($CHCl_3$): λ_{max} (ε, $M^{-1}cm^{-1}$) = 256 (8.03×10^4), 274 (6.76×10^4), 429 (4.45×10^4) nm.

Physical Measurements: FTIR spectra were recorded with a Bruker Vertex 70 FTIR spectrometer in transmission mode at room temperature with a resolution of 2 cm^{-1} and 32 scans in the window 400–4000 cm^{-1} for mid-IR (MIR) and with a resolution of 2 cm^{-1} and 64 scans in the region 180–670 cm^{-1} for far-IR (FIR). UV/Vis absorption spectra were recorded with an Analytik Jena SPECORD 200 spectrophotometer by using a quartz cuvette with a 1 cm path length. Elemental analyses (carbon, hydrogen, nitrogen) were performed by using a Perkin–Elmer CHNS 2400 II elemental analyser. Magnetic measurements were performed on microcrystalline samples of **1** and **2** with a Quantum Design superconducting quantum interference device (SQUID) magnetometer (MPMS-XL). Variable-temperature (2–300 K) direct current (dc) magnetic susceptibility was measured under an applied magnetic field of 0.1 T. All data were corrected for the contribution of the sample holder, and diamagnetism of the complexes was estimated from Pascal's constants.[73]

Crystallographic Structure Determination: The X-ray diffraction data for **1** and **2** were collected with an Oxford Diffraction XCALIBUR E diffractometer equipped with an Eos CCD detector with graphite-monochromated Mo-K_α radiation. The crystals were placed at 40 mm from the CCD detector. The unit-cell determination and data integration were performed with the CrysAlis package of Oxford Diffraction.[74] All structures were solved by direct methods by using SHELXS-97 and refined by full-matrix least-squares on F_o^2 with SHELXL-97[75] with anisotropic displacement parameters for non-hydrogen atoms. All H atoms attached to carbon atoms were inserted in idealised positions (d_{CH} = 0.96 Å) by using the riding model with their isotropic displacement parameters fixed at 120% of that of their riding atom. Positional parameters of the H atoms attached to N atoms were obtained from difference Fourier syntheses and verified by the geometric parameters of the corresponding hydrogen bonds. Most of the atoms from disiloxane moieties in the two structures as well as the counteranions Cl^- in **1** showed quite large thermal ellipsoids; therefore, disorder models in combination with the available tools (PART, DFIX, and SADI) of SHELXL-97 were applied to better fit the electron density. The Si, O and N atoms with fractional site occupancies were refined isotropically. The main crystallographic data together with refinement details are summarised in Table 3.

CCDC-942438 (for **1**) and -942439 (for **2**) contain the supplementary crystallographic data for this paper. These data can be obtained free of charge from The Cambridge Crystallographic Data Centre via www.ccdc.cam.ac.uk/data_request/cif.

Thermogravimetric measurements (TGA) were performed with a Mettler Toledo TGASDTA851e derivatograph in a 20 mL min^{-1} nitrogen stream in the temperature range 25–900 °C and at a heating rate of 10 K min^{-1}. The operational parameters were kept constant for both samples to obtaining comparable data. The magnetic susceptibility (χ) of samples **1** (Mn^{II}_2) and **2** (Mn^{II}_2 + Mn^{II}) has

Table 3. Crystallographic data, details of data collection and structure refinement for **1** and **2**.

	1	**2**
Empirical formula	$C_{76}H_{133}Cl_3Mn_2N_8O_{11}Si_8$	$C_{84.5}H_{141.3}Cl_{7.5}Mn_3N_{12}O_{8.4}Si_8$
Fw	1775.85	2115.21
Space group	$P2_1/n$	$P2_1/c$
a [Å]	16.359(5)	17.5399(8)
b [Å]	24.271(5)	29.9176(9)
c [Å]	28.770(5)	25.0021(6)
β [°]	106.611(5)	92.122(3)
V [Å^3]	10946(4)	13110.9(8)
Z	4	4
$\rho_{calcd.}$ [g cm^{-3}]	1.078	1.072
Crystal size [mm]	0.25× 0.25× 0.10	0.30× 0.10× 0.10
T [K]	200	150
μ [mm^{-1}]	0.439	0.555
$\theta_{min}/\theta_{max}$ [°]	1.83/25.00	3.00/25.03
R_1[a] [$I>2\sigma(I)$]	0.0937	0.0988
wR_2[b] (all data)	0.3001	0.2952
GOF[c]	1.035	1.096

[a] $R1 = \Sigma||F_o| - |Fc||/\Sigma|F_o|$. [b] $wR2 = \{\Sigma[w(F_o^2 - F_c^2)^2]/\Sigma[w(F_o^2)^2]\}^{1/2}$. [c] GOF = $\{\Sigma[w(F_o^2 - F_c^2)^2]/(n-p)\}^{1/2}$; n is the number of reflections and p is the total number of parameters refined.

been measured in the 2–300 K range with a SQUID magnetometer.

The electrochemical experiments were performed with an EG&G PAR 273A potentiostat/galvanostat connected to a personal computer through a GPIB interface. Cyclic voltammetry (CV) studies were undertaken in 0.2 M [nBu$_4$N][BF$_4$]/CH$_3$CN at a platinum disc working electrode (d = 0.5 mm) and at room temperature. Controlled-potential electrolyses (CPE) were performed in electrolyte solutions with the above-mentioned composition in a three-electrode H-type cell. The compartments were separated by a sintered glass frit and equipped with platinum gauze working and counterelectrodes. For both CV and CPE experiments, a Luggin capillary connected to a silver wire pseudoreference electrode was used to control the working electrode potential. A Pt wire was employed as the counterelectrode for the CV cell. The CPE experiments were monitored regularly by cyclic voltammetry to ensure that here was no significant potential drift during the electrolyses. Owing to strong and fast electrode passivation, it was not possible to perform extensively the CPEs, even with frequent electrode cleaning. The solutions were saturated with N_2 by bubbling this gas before each run, and the redox potentials of the complexes were measured by CV in the presence of ferrocene as the internal standard, and their values are quoted relative to the SCE by using the [Fe(η^5-C$_5$H$_5$)$_2$]$^{0/+}$ redox couple ($E^{ox}_{1/2}$ = 0.45 V vs. SCE).[76]

Catalytic Studies: Typical procedures and product analysis: Oxidation reactions of the alcohols were performed in sealed cylindrical Pyrex tubes under focused microwave irradiation as follows: the alcohol (5 mmol), catalyst **1** or **2** (1–70 μmol) and a 70% aqueous solution of tBuOOH (TBHP, 10 mmol, 688 μL) were introduced into the tube. The tube was then placed in the microwave reactor, and the system was left to stir under irradiation (10 W) for 0.5–15 h at 50–90 °C. After the solution had cooled to room temperature, benzaldehyde (internal standard; 300 μL) and CH$_3$CN (to extract the substrate and the organic products from the reaction mixture; 5 mL) were added. The obtained mixture was stirred for 10 min and then a sample (1 μL) was taken from the organic phase and analysed by GC by using the internal standard method.

Gas chromatographic (GC) measurements were performed with a FISONS Instruments GC 8000 series gas chromatograph with a flame ionisation detector (FID) and a capillary column (DB-WAX, column length: 30 m; internal diameter: 0.32 mm). The injection temperature was 240 °C. The initial temperature of the column was maintained at 120 °C for 1 min, then increased by 10 °C/min to 200 °C and held at this temperature for 1 min. Helium was used as the carrier gas.

Supporting Information (see footnote on the first page of this article): TGA curves for **1** and **2**.

Acknowledgments

This research was financially supported by the European Regional Development Fund, Sectoral Operational Programme "Increase of Economic Competitiveness", Priority Axis 2 (SOP IEC-A2-O2.1.2-2009-2, ID 570, COD SMIS-CSNR: 12473, Contract 129/2010-PO-LISILMET) and by the Foundation for Science and Technology (FCT), Portugal, Project Pest-OE/QUI/UI0100/2013. One of the authors (A. A.) acknowledges the financial support of the European Social Fund (Cristofor I. Simionescu Postdoctoral Fellowship Programme, ID POSDRU/89/1.5/S/55216), Sectoral Operational Programme Human Resources Development 2007−2013.

[1] a) C. S. Mullins, V. L. Pecoraro, *Coord. Chem. Rev.* **2008**, *252*, 416–443; b) G. Ambrosi, M. Formica, V. Fusi, L. Giorgi, M. Micheloni, *Coord. Chem. Rev.* **2008**, *252*, 1121–1152; c) G. N. George, R. C. Prince, S. P. Cramer, *Science* **1989**, *243*, 789–791; d) O. Pouralimardan, A. C. Chamayou, C. Janiak, H. Hosseini-Monfared, *Inorg. Chim. Acta* **2007**, *360*, 1599–1608; e) I. C. Szigyártóa, L. Szabób, L. I. Simándia, *J. Mol. Catal. A* **2013**, *372*, 66–71; f) G. A. van Albada, A. Mohamadou, W. L. Driessen, R. De Gelder, S. Tanase, J. Reedijk, *Polyhedron* **2004**, *23*, 2387–2391; g) P. Huang, J. Högblom, M. F. Anderlund, L. Sun, A. Magnuson, S. Styring, *J. Inorg. Biochem.* **2004**, *98*, 733–745.

[2] a) K. Wieghardt, *Angew. Chem.* **1989**, *101*, 1179; *Angew. Chem. Int. Ed. Engl.* **1989**, *28*, 1153–1172; b) R. M. Fronko, J. E. Penner-Hahn, C. J. Bender, *J. Am. Chem. Soc.* **1988**, *110*, 7554–7555; c) Y. Kono, I. Fridovich, *J. Biol. Chem.* **1983**, *258*, 6015–6019; d) H. Sakiyama, H. Kawa, R. Isobe, *J. Chem. Soc., Chem. Commun.* **1993**, 882–884.

[3] Y.-T. Li, C.-W. Yan, D.-Z. Liao, *Transition Met. Chem.* **1998**, *23*, 245–248.

[4] B. H. M. Mruthyunjayaswamy, Y. Jadegoud, O. B. Ijare, S. G. Patil, S. M. Kudari, *Transition Met. Chem.* **2005**, *30*, 234–242.

[5] M.-M. Miao, D.-Z. Liao, Z.-H. Jiang, G.-L. Wang, *Transition Met. Chem.* **1995**, *20*, 399–401.

[6] B. Mabad, P. Cassoux, J.-P. Tuchagues, D. N. Hendrickson, *Inorg. Chem.* **1986**, *25*, 1420–1431.

[7] N. Mangayarkarasi, M. Prabhakar, P. S. Zacharias, *Polyhedron* **2002**, *21*, 925–933.

[8] P. Guerriero, S. Tamburini, P. A. Vigato, *Coord. Chem. Rev.* **1995**, *139*, 17–243.

[9] P. Zanello, S. Tamburini, P. A. Vigato, G. A. Mazzocchin, *Coord. Chem. Rev.* **1987**, *77*, 165–273.

[10] S. Kita, H. Furutachi, H. Okawa, *Inorg. Chem.* **1999**, *38*, 4038–4045.

[11] H. Furutachi, A. Ishida, H. Miyasaka, N. Fukita, M. Ohba, H. Okawa, M. Koikawa, *J. Chem. Soc., Dalton Trans.* **1999**, 2441–2450.

[12] S. Ryan, H. Adams, D. E. Fenton, M. Becker, S. Schindler, *Inorg. Chem.* **1998**, *37*, 2134–2140.

[13] S. K. Dutta, J. Ensling, R. Werner, U. Florke, W. Hasse, P. Gütlich, K. Nag, *Angew. Chem.* **1997**, *109*, 107–110; *Angew. Chem. Int. Ed. Engl.* **1997**, *36*, 152–155.

[14] S. S. Tandon, L. K. Thompson, J. N. Bridson, C. Benelli, *Inorg. Chem.* **1995**, *34*, 5507–5515.

[15] H. Okawa, S. Kida, *Bull. Chem. Soc. Jpn.* **1972**, *45*, 1759–1764.

[16] D. Das, C. P. Cheng, *J. Chem. Soc., Dalton Trans.* **2000**, 1081–1086.
[17] S. R. Korupoju, P. S. Zacharias, *Chem. Commun.* **1998**, 1267–1268.
[18] S. R. Korupoju, N. Mangayarkarasi, S. Ameerunisha, E. J. Valente, P. S. Zacharias, *J. Chem. Soc., Dalton Trans.* **2000**, 2845–2852.
[19] a) N. A. Illán-Cabeza, F. Hueso-Urenã, M. N. Moreno-Carretero, J. M. Martínez-Martos, M. J. Ramírez-Expósito, *J. Inorg. Biochem.* **2008**, *102*, 647–655; b) M. Palaniandavar, M. Velusamy, R. Mayilmurugan, *J. Chem. Sci.* **2006**, *118*, 601–610; c) F. Madeira, S. Barroso, S. Namorado, P. M. Reis, B. Royo, A. M. Martins, *Inorg. Chim. Acta* **2012**, *383*, 152–156; d) S. R. Doctrow, K. Huffman, C. B. Marcus, G. Tocco, E. Malfroy, C. A. Adinolfi, H. Kruk, K. Baker, N. Lazarowych, J. Mascarenhas, B. Malfroy, *J. Med. Chem.* **2002**, *45*, 4549–4558; e) H. Golchoubian, L. Rostami, B. Kariuki, *Polyhedron* **2010**, *29*, 1525–1533.
[20] A. J. Atkins, D. Black, R. L. Finn, A. Marín-Becerra, A. J. Blake, L. Ruíz-Ramírez, W. S. Li, M. Schröder, *Dalton Trans.* **2003**, 1730–1737.
[21] J. Gradinaru, A. Forni, Y. Simonov, M. Popovici, S. Zecchin, M. Gdaniec, D. E. Fenton, *Inorg. Chim. Acta* **2004**, *357*, 2728–2736.
[22] P. A. Vigato, S. Tamburini, *Coord. Chem. Rev.* **2004**, *248*, 1717–2128.
[23] M. Paluch, J. Lisowski, T. Lis, *Dalton Trans.* **2006**, 381–388.
[24] S. Khanra, T. Weyhermüller, E. Bill, P. Chaudhuri, *Inorg. Chem.* **2006**, *45*, 5911–5923.
[25] N. Sekine, T. Shiga, M. Ohba, H. Okawa, *Bull. Chem. Soc. Jpn.* **2006**, *79*, 881–885.
[26] J.-Z. Wu, E. Bouwman, A. M. Mills, A. L. Spek, J. Reedijk, *Inorg. Chim. Acta* **2004**, *357*, 2694–2702.
[27] Z. M. Wang, M. Yuan, Z. He, C.-S. Liao, C.-H. Yan, *Acta Chim. Sinica* **2000**, *58*, 1615–1625.
[28] M. Goher, M. A. M. Abu-Youssef, F. A. Mautner, *Polyhedron* **1993**, *12*, 1751–1756.
[29] a) A. Garoufis, S. Kasselouri, S. Boyatzis, C. P. Raptopoulou, *Polyhedron* **1999**, *18*, 1615–1620; b) I. Romero, M.-N. Collomb, A. Deronzier, A. Llobet, E. Perret, J. Pécaut, L. Le Pape, J.-M. Latour, *Eur. J. Inorg. Chem.* **2001**, 69–72.
[30] R. Wortmann, U. Flörke, B. Sarkar, V. Umamaheshwari, G. Gescheidt, S. Herres-Pawlis, G. Henkel, *Eur. J. Inorg. Chem.* **2011**, 121–130.
[31] A. Soroceanu, M. Cazacu, S. Shova, C. Turta, J. Kožišek, M. Gall, M. Breza, P. Rapta, T. C. O. Mac Leod, A. J. L. Pombeiro, J. Telser, A. A. Dobrov, V. B. Arion, *Eur. J. Inorg. Chem.* **2013**, 1458–1474.
[32] I. Yilgor, J. E. McGrath, Polysiloxane Containing Copolymers: A Survey of Recent Developments, in: *Advances in Polymer Science*, vol. 86, *Polysiloxane Copolymers/Anionic Polymerization* (Ed.: R. Stumpe), Springer-Verlag, Berlin, **1988**, p. 1–86.
[33] a) K. Nakamoto, *Infrared and Raman Spectra of Inorganic and Coordination Compounds*, John Wiley & Sons, New York, **1986**; b) S. Brooker, V. McKee, W. B. Shepard, L. K. Panell, *J. Chem. Soc., Dalton Trans.* **1987**, 2555–2562.
[34] B. H. M. Mruthyunjayaswamy, O. B. Ijare, Y. Jadegoud, *J. Braz. Chem. Soc.* **2005**, *16*, 783–789.
[35] M. Sönmez, M. Çelebi, I. Berber, *Eur. J. Med. Chem.* **2010**, *45*, 1935–1940.
[36] S. M. Annigeri, A. D. Naik, U. B. Gangadharmath, V. K. Revankar, V. B. Mahale, *Transition Met. Chem.* **2002**, *27*, 316–320.
[37] Z. Chu, W. Huang, *Inorg. Chem. Commun.* **2008**, *11*, 1166–1169.
[38] S. Mohanta, K. K. Nanda, R. Werner, W. Haase, A. K. Mukherjee, S. K. Dutta, K. Nag, *Inorg. Chem.* **1997**, *36*, 4656–4664.
[39] B. K. Shin, M. Kim, J. Han, *Polyhedron* **2010**, *29*, 2560–2568.
[40] W. Park, J.-H. Cho, H.-I. Lee, M. Park, M. S. Lah, D. Lim, *Polyhedron* **2008**, *27*, 2043–2048.
[41] J.-W. Zhang, H.-S. Wang, Y. Song, *Inorg. Chem. Commun.* **2011**, *14*, 56–60.
[42] B.-K. Shin, Y. Kim, M. Kim, J. Han, *Polyhedron* **2007**, *26*, 4557–4566.
[43] Z.-M. Hao, X.-M. Zhang, H.-S. Wu, S. W. Ng, *Sect. E Struct. Rep. Online* **2005**, *61*, m973.
[44] S. Onaka, L. Hong, M. Ito, T. Sunahara, H. Imai, K. Inoue, *J. Coord. Chem.* **2005**, *58*, 1523–1530.
[45] S. Cromie, F. Launay, V. McKee, *Chem. Commun.* **2001**, 1918–1919.
[46] P. E. Kruger, F. Launay, V. McKee, *Chem. Commun.* **1999**, 639–640.
[47] A. C. Raimondi, P. B. Hitchcock, G. J. Leigh, F. S. Nunes, *J. Chem. Crystallogr.* **2002**, *32*, 363–367.
[48] S. S. Tandon, L. K. Thompson, J. N. Bridson, M. Bubenik, *Inorg. Chem.* **1993**, *32*, 4621–4631.
[49] S. Dutta, P. Biswas, *J. Mol. Struct.* **2011**, *996*, 31–37.
[50] J. M. K. Gebbink, R. T. Jonas, C. R. Goldsmith, T. D. P. Stack, *Inorg. Chem.* **2002**, *41*, 4633–4641.
[51] T.-F. Liu, D.-Z. Gao, H.-K. Lin, S.-R. Zhu, Z.-M. Wang, H.-G. Wang, X.-B. Leng, *Transition Met. Chem.* **2004**, *29*, 296–300.
[52] C. M. Coates, K. Hagan, C. A. Mitchell, J. D. Gorden, C. R. Goldsmith, *Dalton Trans.* **2011**, *40*, 4048–4053.
[53] W. Park, M. H. Shin, J. H. Chung, J. Park, M. S. Lah, D. Lim, *Tetrahedron Lett.* **2006**, *47*, 8841–8845.
[54] V. K. Sharma, S. Srivastava, *Turk. J. Chem.* **2006**, *30*, 755–767.
[55] a) O. Kahn, *Molecular Magnetism*, VCH Publishers, New York, **1993**; b) R. Carlin, *Magnetochemistry*, Springer, Berlin, **1986**.
[56] P. L. Pawlak, M. Panda, R. Loloee, B. Kucera, J.-P. Costes, J.-P. Tuchagues, F. A. Chavez, *Dalton Trans.* **2011**, *40*, 2926–2931.
[57] B. K. Shin, Y. Kim, M. Kim, J. Han, *Polyhedron* **2007**, *26*, 4557–4566.
[58] B. Bräuer, D. Schaarschmidt, C. Flohrer, T. Rüffer, S. Tripke, A. Hildebrandt, L. Sorace, H. Lang, *Inorg. Chim. Acta* **2011**, *365*, 277–281.
[59] a) A. Loupy (Ed.), *Microwaves in Organic Synthesis* Wiley/VCH, Weinheim, Germany, **2002**; b) J. P. Tierney, P. Lidström (Eds.), *Microwave Assisted Organic Synthesis*, Blackwell Publishing/CRC Press, Oxford, UK, **2005**; c) D. Dallinger, C. O. Kappe, *Chem. Rev.* **2007**, *107*, 2563–2591; d) Y. Sun, L.-C. Wang, Y.-M. Liu, Y. Cao, H.-Y. He, K.-N. Fan, *Catal. Commun.* **2007**, *8*, 2181–2185; e) A. De La Hoz, A. Diaz-Ortiz, A. Moreno, *Chem. Soc. Rev.* **2005**, *34*, 164–167.
[60] M. N. Kopylovich, Y. Y. Karabach, M. F. C. Guedes da Silva, P. J. Figiel, J. Lasri, A. J. L. Pombeiro, *Chem. Eur. J.* **2012**, *18*, 899–914.
[61] R. R. Fernandes, J. Lasri, M. F. C. Guedes da Silva, J. A. L. Silva, J. J. R. Fraústo da Silva, A. J. L. Pombeiro, *J. Mol. Catal. A* **2011**, *351*, 100–111.
[62] J. Lasri, M. J. F. Rodriguez, M. F. C. Guedes da Silva, P. Smolenski, M. N. Kopylovich, J. J. R. Fraústo da Silva, A. J. L. Pombeiro, *J. Organomet. Chem.* **2011**, *696*, 3513–1520.
[63] P. J. Figiel, M. N. Kopylovich, J. Lasri, M. F. C. Guedes da Silva, J. J. R. Fraústo da Silva, A. J. L. Pombeiro, *Chem. Commun.* **2010**, *46*, 2766–2768.
[64] a) A. Dijksman, I. W. C. E. Arends, R. A. Sheldon, *Org. Biomol. Chem.* **2003**, *1*, 3232–3237; b) R. A. Sheldon, I. W. C. E. Arends, *J. Mol. Catal. A* **2006**, *251*, 200–214; c) R. A. Sheldon, I. W. C. E. Arends, *Adv. Synth. Catal.* **2004**, *346*, 1051–1071; d) G. Yang, W. Zhu, P. Zhang, H. Xue, W. Wang, J. Tian, M. Songa, *Adv. Synth. Catal.* **2008**, *350*, 542–546; e) L. Lin, M. Juanjuan, J. Liuyan, W. Yunyang, *J. Mol. Catal. A* **2008**, *291*, 1–4; f) L. Lin, M. Juanjuan, J. Liuyan, W. Yunyang, *Catal. Commun.* **2008**, *9*, 1379–1382; g) S. Striegler, *Tetrahedron* **2006**, *62*, 9109–9114; h) C. Michel, P. Belanzoni, P. Gamez, J. Reedijk, E. J. Baerends, *Inorg. Chem.* **2009**, *48*, 11909–11920; i) P. Gamez, I. W. C. E. Arends, R. A. Sheldon, J. Reedijk, *Adv. Synth. Catal.* **2004**, *346*, 805–811; j) P. Gamez, I. W. C. E. Ar-

ends, J. Reedijk, R. A. Sheldon, *Chem. Commun.* **2003**, *19*, 2414–2415; k) J. S. Uber, Y. Vogels, D. van den Helder, I. Mutikainen, U. Turpeinen, W. T. Fu, O. Roubeau, P. Gamez, J. Reedijk, *Eur. J. Inorg. Chem.* **2007**, *26*, 4197–4206.

[65] a) P. J. Figiel, M. Leskelä, T. Repo, *Adv. Synth. Catal.* **2007**, *349*, 1173–1179; b) P. J. Figiel, A. M. Kirillov, Y. Y. Karabach, M. N. Kopylovich, A. J. L. Pombeiro, *J. Mol. Catal. A* **2009**, *305*, 178–182; c) P. J. Figiel, A. Sibaouih, J. U. Ahmad, M. Nieger, M. T. Räisänen, M. Leskelä, T. Repo, *Adv. Synth. Catal.* **2009**, *351*, 2625–2632; d) J. U. Ahmad, P. J. Figiel, M. T. Räisänen, M. Leskelä, T. Repo, *Appl. Catal. A* **2009**, *371*, 17–21; e) K. T. Mahmudov, M. N. Kopylovich, M. F. C. Guedes da Silva, P. J. Figiel, Y. Yu. Karabach, A. J. L. Pombeiro, *J. Mol. Catal. A* **2010**, *318*, 44–50.

[66] I. N. Moiseeva, A. E. Gekham, V. V. Minin, G. M. Larin, M. E. Bashtanov, A. A. Krasnovskii, I. I. Moiseev, *Kinet. Catal.* **2000**, *41*, 170–182.

[67] J. M. Mattalia, B. Vacher, A. Samat, M. Chanon, *J. Am. Chem. Soc.* **1992**, *114*, 4111–4119.

[68] R. A. Sheldon, *Chem. Commun.* **2008**, *29*, 3352–3365.

[69] R. A. Sheldon, I. W. C. E. Arends, *Adv. Synth. Catal.* **2004**, *346*, 1051–1071.

[70] A. Cecchetto, F. Fontana, F. Minisci, F. Recupero, *Tetrahedron Lett.* **2001**, *42*, 6651–6653.

[71] G. Yang, J. Ma, W. Wang, J. Zhao, X. Lin, L. Zhou, X. Gao, *Catal. Lett.* **2006**, *112*, 83–87.

[72] R. S. Varma, R. K. Saini, R. Dahiya, *Tetrahedron Lett.* **1997**, *38*, 7823–7824.

[73] P. Pascal, *Ann. Chim. Phys.* **1910**, *19*, 5–70.

[74] CrysAlis PRO, Aglient Technologies Ltd., Yarnton, **2011**.

[75] G. M. Sheldrick, *Acta Crystallogr., Sect. A* **2008**, *64*, 112–122.

[76] A. J. L. Pombeiro, M. F. C. G. Silva, M. A. N. D. A. Lemos, *Coord. Chem. Rev.* **2001**, *219*, 53–80.

Received: July 28, 2013
Published Online: November 22, 2013

